Spatial cell fate manipulation of human pluripotent stem cells by controlling the microenvironment using photocurable hydrogel.

Zhe Wang[1,2], Akira Numada[1,2], Fumi Wagai[1], Yusuke Oda[1,2], Masatoshi Ohgushi[1,2], Koichiro Maki[4], Taiji Adachi[4], Mototsugu Eiraku[1,2,3*]

[1]Laboratory of Developmental Systems, Institute for Life and Medical Sciences, Kyoto University, Kyoto, 606-8507, Japan

[2]Department of Polymer Chemistry, Graduate School of Engineering, Kyoto University, Kyoto, 606-8507, Japan

[3]Institute for Advanced Study of Human Biology (WPI-ASHBi), Kyoto University, Yoshida-Konoe-Cho, Sakyo-Ku, Kyoto, 606-8501, Japan

[4]Laboratory of Biomechanics, Institute for Life and Medical Sciences, Kyoto University, Kyoto, 606-8507, Japan

***Corresponding author:** Mototsugu Eiraku, Email Address: eiraku.mototsugu.2u@kyoto-u.ac.jp

Key words: hydrogel, human pluripotent stem cell, differentiation, spatial control

Abstract

Human pluripotent stem cells (hPSCs) sense the surrounding chemical and physical microenvironment and adjust their behavior accordingly. However, current *in vitro* research is mostly conducted in plastic culture wares, which provides an oversimplified microenvironment compared to that *in vivo*. Increasing evidence has highlighted the importance of the physical microenvironment in hPSCs differentiation and maintenance. Here, hPSCs were cultured on homogeneous substrates with specific stiffness. Biocompatible material that allows spatial control of the chemical and mechanical environment for hPSC culture has not yet been developed. Culture substrates that enable flexible manipulation of spatial physical properties can assist the recapitulation of an *in vivo* environment and assist tissue engineering.

We developed a photocurable polyethylene glycol–polyvinyl alcohol (PVA-PEG) hydrogel, which allows spatial control of the surface stiffness and structure at a micrometer level. The developed hydrogel can be functionalized using different extracellular matrix (ECM) proteins. Laminin 511 functionalized PVA-PEG gel supports hPSCs growth and differentiation. Furthermore, by spatially controlling the stiffness of the patterned gel, we could selectively differentiate cells, generating complex patterned structures.

Keywords: Human pluripotent stem cells, microenvironment, differentiation, biocompatible.

Introduction

hPSCs are intensively used in regenerative medicine and developmental biology research. Many types of cells and tissues have been generated from hPSCs, providing a powerful tool for *in vitro* study. However, the current culture system is distinct from the *in vivo* microenvironment, limiting the generation of complex structures *in vitro*. Pluripotent stem cells (PSC) can be cultured for differentiation in either two- or three-dimensional (2D or 3D) condition. 2D culture provides a simple, reproducible, and robust culture condition, and many cell differentiation protocols have been developed in 2D. In contrast, in 3D culture, cells form aggregates that float in the culture medium or are embedded in an ECM

(Gattazzo et al., 2014; Simunovic and Brivanlou, 2017). In both culture systems, stem cells are differentiated by adjusting the composition of the culture medium. 2D culture systems are subject to mechanical constraints on tissue shape because cells are cultured on a rigid culture dish. In contrast, in 3D culture systems, induced tissues are less mechanically constrained and can more freely change their shape. During development, stem cells form organs under weak mechanical constraints through chemical and mechanical signals mediated by tissue-tissue interactions (Simunovic and Brivanlou, 2017). Therefore, to induce functional tissues with appropriate shapes *in vitro*, an ideal environment allows tissue deformation with weak mechanical constraints.

Increasing evidence suggests the importance of physical cues on cell behavior and fate (Candiello et al., 2013; Chen et al., 2020; Keung et al., 2012; Maldonado et al., 2017; Muduli et al., 2017; Musah et al., 2014; Przybyla et al., 2016; Rosowski et al., 2015). Soft substrates and high mechanical tension enhance hPSC mesodermal differentiation (Muncie et al., 2020; Przybyla et al., 2016). Simultaneously, substrate geometry and structures are also critical to complex tissue structure generation (Karzbrun et al., 2021; Warmflash et al., 2014). During development, neighboring cells communicate, sensing the surrounding chemical and mechanical cues, and differentiate accordingly. Eventually, cells gain differentiated cell fate and cooperate to form organs with complex structures. Therefore, it is important to spatially control the microenvironment to generate complex cellular structures. To this end, we aimed to develop a culture substrate with adjustable mechanical properties.

Hydrogels have been used intensively in biomedical research as cell culture substrates due to their mechanical and chemical similarity with the ECM(Tibbitt and Anseth, 2009). Furthermore, hydrogels can be functionalized with different properties, such as photocurability. Photocurable hydrogels based on hyaluronic acid and gelatin have been developed(Chen et al., 2019; Tibbitt and Anseth, 2009). By controlling the light source, gels with different shapes and structures can be generated. However, these gels were used for hPSCs encapsulation, but not for attachment due to poor adhesivity on the synthetic surface of hPSCs (Tibbitt and Anseth, 2009; Virdi and Pethe, 2021). In contrast, some hydrogels allow suitable hPSC attachment, such as polyacrylamide or polydimethylsiloxane (PDMS), that have been used intensively in studies regarding substrate stiffness (Chen et al., 2019;

Chen et al., 2020; Maldonado et al., 2017; Millar-Haskell et al., 2019; Perez-Puyana et al., 2020; Tibbitt and Anseth, 2009). However, they lack flexibility regarding gel structure and mechanical property control. Driven by this discussion, we developed a photocurable hydrogel with ideal hPSCs attachment.

hPSCs attach to the substrate via integrin-ECM protein interactions. Therefore, ECM protein engraftment on the hydrogel is necessary. Previously, ECM protein functionalized PVA could be used for hPSCs culture (Muduli et al., 2017). Polyvinyl alcohol (PVA), a polymer with a simple structure, can form a stable and biocompatible hydrogel upon cross-linking. We used PVA as the backbone and further functionalized PVA to have photocurability and ECM proteins to facilitate hPSCs attachment.

Here, we demonstrated a composite photocurable PVA and PEG hydrogel with adjustable stiffness and shape. Our hydrogel supports hPSCs growth and differentiation, and the differentiation tendency of hPSCs was compared with cells cultured on plastic dishes. Most importantly, we demonstrated that stem cell fate could be spatially manipulated at a micrometer level by controlling the local physical property of substrates.

Results

1. Synthesis and characterization of photocurable PVA-methacrylate hydrogel

To develop a photocurable hydrogel with protein binding ability, we used a denatured Polyvinyl alcohol (PVA-COOH), which contains randomly integrated carboxyl groups as starting material. The carboxyl group in the PVA backbone can be activated by 1-ethyl-3-(3-dimethylaminopropyl) carbodiimide/N-hydroxysuccinimide (NHS/EDC) and further bind with the N end of ECM proteins to allow cell attachment (Fig. 1A). To obtain photocurability, a methacrylate functional group was introduced into the PVA backbone to obtain photocurable PVA-MA. Lithium phenyl-2,4,6-trimethyl-benzoyl phosphonate (LAP) (0.5%) was used as the photoinitiator (Fig. 1B).

Increasing evidence suggests the importance of the diameter of colony and substrate geometry in generating complex tissue *in vitro* (Karzbrun et al., 2021; Warmflash et al.,

2014). However, current micropatterned cultures are typically constructed on glass or plastic cultureware, and their physical property *in vitro* differs from that under *in vivo* conditions. Taking advantage of the flexibility of photoinitiated crosslinkability of our hydrogel, we attempted to develop a patterned culture method using our hydrogel. As seen in Fig. 2C, we generated a spacer with a round hole in the center using PDMS. The spacer was then put on the glass-bottom dish. Hydrogel prefabrication solution was added into the hole and then covered by a coverslip. We then used a direct-exposure photolithography system to initiate patterned UV light to initiate gelation. With this method, we were able to create various-shaped gels at the micrometer level (Fig. 1,C-D). However, we encountered an issue where the PVA-MA gel alone was too soft. Previous research demonstrated that by incorporating 4-arm PEG with different molecular weights and ratios, hydrogels with stiffness ranging from approximately 500 Pa to 500 kPa could be obtained(Lee et al., 2014). Therefore, we introduced 4-arm PEG to create a composite hydrogel. Furthermore, we could precisely control the stiffness of the PVA-PEG composite hydrogel by adjusting the dosage of UV irradiation. In this study, we utilized a mixture of 3% PVA and 15% 5K 4-arm PEG, as it provided us with a soft, in vivo-like stiffness and clear boundaries when generating gel patterns (Fig. 1, D-E). Consequently, we have developed a photocurable hydrogel substrate with adjustable stiffness, ranging from soft (~700 Pa) to hard (~6 kPa), achieved through the combination of 3% PVA and 15% 5K 4-arm PEG."

The crosslink density not only influences the stiffness of the hydrogel but also determines the mesh size of the hydrogel network. This can potentially impact cells by affecting the diffusion of proteins in the culture medium. Therefore, we investigated the diffusivity of fluorescent molecules with varying molecular weights in gels with different stiffness levels.

As illustrated in Fig. 1,F and Fig. S1, molecules with a molecular weight of 4 kDa or larger were unable to diffuse within both hard and soft hydrogels. However, when using a molecule with a molecular weight of 1.4 kDa, it was capable of diffusing into both hard and soft gels, with the softer gel exhibiting higher diffusivity.

To assess the protein-binding capability of PVA-MA, we incubated both activated and non-activated PVA-MA with a fluorescent protein (Fig. 1, G). Following incubation, we measured the fluorescence intensity to quantify the hydrogel's protein-binding capacity.

Activated gel demonstrated a significantly higher fluorescent signal (Fig. 1H), approximately 20 times greater than that of the non-activated hydrogel and 1.2 times greater than conventional coating methods on a glass surface. This result indicates successful protein binding to our hydrogel.

2. PVA-PEG gels support hPSC survival and outgrowth while maintaining pluripotency.

Next, we tested whether our gel supports hPSC growth. We generated two types of gels: one with a stiffness of approximately 6 kPa (hard) and another with a stiffness of around 700 Pa (soft). These gels were then activated and coated with laminin 511 as ECM proteins for hPSC culture.

To analyze cell proliferation, we developed a nucleus reporter H2B-mCherry hPSCs line that enabled us to track cell movements and conduct cell cycle analysis. H2B-mCherry-labeled cells were seeded on culture dishes or hydrogels, and live imaging was conducted to monitor cell nuclear division. We found that cells cultured on the gel exhibited a similar proliferation rate compared to those cultured on glass-bottom dishes (Fig. 2A). Cells on the softer gel displayed slightly longer cell cycles, consistent with previous reports(Guo et al., 2020; Shao et al., 2015).

Immunofluorescence (IF) and transcriptome analysis indicated that hPSCs cultured on both hard and soft hydrogels maintained their pluripotency within one passage. This was evidenced by the expression of pluripotent markers (SOX2, OCT4, NANOG) in Day 6 cultures on the gel (Fig. 2B, FigS2). These results suggest that pluripotency and proliferation of hESCs can be sustained on hydrogels, at least within the observed time window (6 days).

It was previously known that hPSCs tend to lose nuclear-localized YAP when cultured on softer substrates, which is a key mechanosensing gene involved in various biological processes. Therefore, we investigated the impact of our gel on YAP localization. Cells on hard gel and conventional glass dishes exhibited clear nuclear-localized YAP, while soft gel did not (Fig. 2C, Fig. S3A-B). This nuclear localized YAP cannot be inhibited by the Rho-kinase inhibitor Y-27632(Fig. S3A-B). Interestingly, cells on the hard gel also displayed nuclear YAP, even though it has a relatively soft stiffness of 6kPa. This is likely due to our gel's high

protein binding capacity, which results in a dense ECM ligand (Fig. 1G-H), thus promoting nuclear YAP, as observed previously.(Kechagia et al., 2023; Lee et al., 2019; Stanton et al., 2019).

3. Soft substrate enhances Nodal signaling and the formation of beta-catenin while maintaining pluripotency.

We assessed the impact of hydrogel stiffness on hPSCs gene expression. At Day 4, hPSCs cultures on hard gel (~6kPa), soft gel (~700Pa), and glass-bottom dishes were collected for RNA-seq analysis. We assembled a total of 34,032 transcripts. Among these, 1,288 genes were upregulated on the softer gel compared to the hard gel (Fig. 3A). Notably, pluripotent genes like SOX2, OCT3/4, and NANOG showed similar expression in all samples, consistent with immunostaining results (Fig. 2B, Fig. S2). In contrast, endoderm-related genes such as NODAL, ANXA1, CER1, FOXA2, LEFTY1, LEFTY2, SMAD7, SERPINE1, and TIMP4 were upregulated in both softer and harder gels compared to culture dishes(Fig. 3B-C). The harder gel exhibited slightly higher endoderm gene expression compared to the soft gel (Fig. S2). Compared to culture dishes, Gene Ontology (GO) analysis indicated that soft hydrogels enriched genes related to: Formation of the beta-catenin, cell morphogenesis, endoderm development, Degradation of the extracellular matrix (Fig. 4D). Hard gel enriched gene groups related to: cell morphogenesis involved in differentiation, endoderm development, tissue morphogenesis (Fig. 4E). Additionally, the harder gel displayed higher expression of YAP downstream genes compare with soft gel, consistent with our immunofluorescence (IF) results (Fig. 2C, Fig. S2).

During embryonic gastrulation, NODAL signaling is induced posteriorly by Wnt3a, which, in turn, is triggered by BMP4. NODAL signaling further amplifies itself. The localized posterior NODAL and WNT signaling jointly initiate the formation of the primitive streak, leading to the subsequent generation of mesendoderm(Evseenko et al., 2010; Loh et al., 2014; Loh et al., 2016; Martyn et al., 2019; Martyn et al., 2018).

Previous reports have shown that culturing hPSCs on a 3kPa substrate upregulates the long noncoding RNA (LncRNA) LINC00458 and LINC01356 were upregulated, and LINC00458 interacts with SMAD 2/3, a downstream effector of Nodal, thereby promoting

endoderm differentiation(Chen et al., 2020). We found these genes also upregulated in cells cultured on the soft and hard gels (Fig. S2).

Additionally, previous research has demonstrated that when hESCs are cultured on a 400Pa hydrogel, protein level of β-catenin was upregulated. This upregulation enhances Wnt-dependent mesoderm differentiation upon treatment with morphogens. In contrast, on a stiff hydrogel matrix (60kPa), β-catenin degradation is promoted, leading to the inhibition of differentiation (Przybyla et al., 2016). This aligns with our GO analysis of the soft gel, where the top-enriched gene group is 'Formation of the beta-catenin:TCF transactivating complex' (R-HSA-201722) (Fig. 3D).

In summary, hPSCs cultured on both soft and hard gels exhibited upregulated NODAL signaling, possibly mediated by LINC00458 and SMAD 2/3 upregulation. Cells on the hard gel expressed higher YAP downstream genes and slightly higher but not significantly different endoderm-related genes, likely due to the preferred stiffness range for endoderm differentiation (Chen et al., 2020; Maldonado et al., 2017; Srivastava et al., 2023). Furthermore, in addition to exhibiting similar trends as the hard gel, the soft gel also showed enhanced formation of beta-catenin. Importantly, both the hard and soft gels, maintained pluripotency within the observed time window, as evidenced by pluripotent gene expression (Fig. S2).

4. hPSCs can be differentiated into all germ layers on PVA-PEG gel

Given the fact that our gel with different stiffness levels has varying impacts on the transcriptome, we next evaluated how our gel would affect stem cell differentiation. Cells passaged on the PS dish were collected and seeded on the hard and soft PVA-PEG gel and subsequently differentiated towards 3 germ layers following previously reported protocols (D'Amour et al., 2005; Evseenko et al., 2010; Loh et al., 2016; Surmacz et al., 2012).

For neural ectoderm (NE), hPSCs were differentiated using the previously reported dual SMAD inhibition method (Chambers et al., 2009). After 6 days of differentiation, cells on both dish and gel cultures largely expressed the NE markers, PAX6 and OTX2, suggesting successful NE differentiation (Fig. 4A Fig. S4A). qPCR suggests cells differentiated on the dish cultures have similar expression of NE genes than on hard and soft gel which is consistent with the previous report when they compared NE differentiation on hydrogel (700Pa, 75 kPa

and 300 kPa) and culture dish (2.28–3.28 GPa)(Fig. S4A) (Keung et al., 2012; Maldonado et al., 2017).

For definitive endoderm (DE), cells were first differentiated to the anterior primitive streak (APS) for 24 h and then towards DE (D'Amour et al., 2005; Evseenko et al., 2010). As Fig. 4B shows, cells on both culture dishes and gels were successfully differentiated, supported by the NE marker SOX17 expression in most cells. Interestingly, qPCR revealed a notably enhanced expression of APS and DE-related genes on hard and soft gel compared with culture dish. But there is no statistically significant difference between them (Fig. S4B),.

For Mesodermal development, the paraxial mesoderm (PM) and lateral plate mesoderm (LPM) fates separate at the early stages of differentiation, therefore we tested both.

For LPM, hESCs cells were differentiated toward mid primitive streak (MPS) for 24 h and then towards LPM for 24 h following the previously reported protocol (Loh et al., 2016). IF suggested that the differentiation both on the gel and culture dish was successful (Fig. 4C). Cells differentiated on gels expressed a higher level of *HAND1* and *ISL1* but expressed a lower level of *NKX2.5*(Fig. S4C),

For PM, hESCs were differentiated towards APS for 24 h, and then APS was directed towards PM for 24 h (Loh et al., 2016). Although soft substrate was shown to enhance mesendoderm fate (Chen et al., 2020; Przybyla et al., 2016), IF and qPCR reflected similar expression of LPM markers(Fig 4D, FigS4D)

For both PM and LPM, qPCR revealed different differentiation efficiencies on the gel compared to conventional dishes, yet the changes remained within a similar range (less than a 2-fold change). We hypothesized that the extended differentiation processes of PM and LPM, involving multiple steps (APS to PM or MPS to LPM), could mitigate the substrate's impact on mesoderm differentiation. Therefore, we next differentiated hPSCs into this early mesoderm population using BMP4, as previously reported(Evseenko et al., 2010; Przybyla et al., 2016). Indeed, when compared with a conventional dish, the mesoderm markers T and MESP1 showed a 6 and 10-fold upregulation on hard gel comparing on glass dish (Fig. S4E).

5. Manipulating cell fate of hPSCs on the patterned gel by controlling substrate stiffness

Soft substrates have been shown to enhance mesoderm differentiation(Pagliari et al., 2021; Przybyla et al., 2016). Given that our gel allows for spatially adjustable stiffness, we wondered if it is possible to manipulate stem cell fate locally by creating soft regions within the hydrogel.

We hypothesized that if we generate locally soft patterned hydrogel and we could selectively differentiate cells on the soft part towards the early mesoderm. We first generated soft and hard patterned gel and differentiated hPSCs on gels towards the mesoderm by administrating 10 ng/mL BMP4 and bFGF(Evseenko et al., 2010; Przybyla et al., 2016) in differentiating medium(Fig. S5A). After 24 h of differentiation, cells on the soft gel were differentiated to a mesendoderm fate which was indicated by the expression of mesodermal and primitive streak marker T. Most cells on hard gels do not express T, except a few cells on the edge (Fig. S5B), probably due to weaker cell-cell junction and higher tension(Muncie et al., 2020; Przybyla et al., 2016). These results indicate that it is possible to manipulate stem cell fate by adjusting the stiffness of the hydrogel. Since the stiffness of the gel is easily controlled by UV dosage, we next generated a hydrogel with locally different stiffness using a patterned irradiating system (Fig. 5A, Fig. S5C). We controlled the stiffness of the gel using UV dosage and created a hydrogel with locally varying stiffness through a patterned irradiation system. We confirmed the stiffness distribution in the gel pattern, which revealed a clear boundary between soft and hard areas (Fig. 5A). The median stiffness was 116 Pa for the soft part and 2715 Pa for the hard part (Fig. 5B). Both soft and hard areas were softer than the non-patterned gel, likely due to the leakage of photo-initiator into the non-irradiated area.

We seeded hPSCs on a patterned hydrogel, with one half being hard and the other half soft. After 24 hours of differentiation towards early mesoderm, cells in the hard areas remained pluripotent, as indicated by positive SOX2 and negative T assays. Conversely, cells in the softer areas exhibited early mesodermal fate, as shown by their T expression and the absence of SOX2 expression (Fig. SC), even though they were differentiated in the same dish. We calculated the number of T+ cells per area based on the IF image, as demonstrated in Fig.

S5D, and found that cells on the softer gel pattern had a significantly higher (~200 times) rate of T+ cells. Fig. S5E illustrates the distribution of T+ cells per area in both soft and hard areas of the same patterned gel.

Despite the significant difference in T^+ cell number after 24 h of differentiation, we found that cells on both the hard and soft areas became T^+ after 48hr differentiation in the presence of BMP4 and bFGF. Therefore, we next tested if it is possible to maintain the patterned differentiation by administering a pulse of morphogen stimulation. hPSCs were seeded on hydrogel patterns and cultured in the pluripotency maintenance medium. BMP4 and bFGF (10 ng/mL each) were directly added into the maintenance medium for 24 h and then withdrawn by medium change (Fig. 5C). The cells were cultured in a maintenance medium for another 48 h. As Fig. 5D shows, cells on the soft gel are largely T positive, while only a few T-positive cells on hard gels. On the patterned gels, T-positive cells are mostly restricted in soft areas and lose *SOX2* expression. In contrast, cells cultured on hard gels mostly retained the *SOX2* expression (Fig. 5E). These data suggest that we could selectively differentiate cells by spatially controlling the hydrogel stiffness.

We investigated how soft gels promote early mesoderm differentiation. During gastrulation, BMP4 triggers downstream Wnt signaling, inducing mesoderm formation (Martyn et al., 2018). RNA-seq analysis also demonstrated enhanced β-catenin formation on the soft gel substrate (Fig. 3D), a key component of the Wnt signaling pathway. This aligns with a prior study (Przybyla et al., 2016) where cells cultured on a softer (400Pa) gel exhibited stable adherens junctions, increased β-catenin expression, and inhibited β-catenin degradation. Conversely, β-catenin destabilized and degraded in cells on a harder (60kPa) gel. Consequently, cells on the softer gel exhibited heightened Wnt signaling sensitivity to BMP4-induced differentiation. To investigate the role of Wnt/β-catenin signaling, we conducted perturbation experiments. Initially, we differentiated cells on locally soft and hard gel patterns with BMP and bFGF in the presence of 2.5 μM IWP2, an inhibitor of Wnt secretion. This led to a complete abolition of differentiation, even when extended for 48 hours (Fig 6A).

Conversely, when we employed the GSK3 inhibitor CHIR99201 to inhibit β-catenin degradation, differentiation occurred in both hard and soft areas even without the addition

of morphogens. This differentiation occurred without a significant time difference between soft and hard region, unlike when differentiated with BMP (Fig. 6A-B, Fig. S6A-C Movie 1.). These results suggest a crucial involvement of Wnt/β-catenin signaling in the observed stem cell fate differences on the gel pattern.

We also observed a downregulation of YAP nuclear trafficking on softer gels. YAP serves as a major mechanical sensor and has been shown to influence hESCs differentiation into various germ layers, including mesoderm. Numerous studies have reported that YAP signaling activation has a negative impact on SMAD2/3 and Wnt signaling, thereby negatively regulating mesoderm differentiation(Estaras et al., 2017; Pagliari et al., 2021; Qin et al., 2016; Srivastava et al., 2023; Stronati et al., 2022). Conversely, inhibiting YAP nuclear trafficking promotes Wnt signaling and triggers gastrulation-like differentiation (Srivastava et al., 2023). Therefore, we investigated the YAP and β-catenin within our system.

As shown in the Fig. 6E, on the hard part of the gel pattern, YAP still exhibited visible nuclear localization, while cells on the soft part displayed the opposite pattern (Fig. 6C). This aligns with the results we obtained on the non-patterned gel (Fig. 2C). Similarly, soft gel also showed stronger β-catenin staining(Fig. 2C), consistent with previous reports, a soft substrate promoted β-catenin accumulation and downregulated degradation (Przybyla et al., 2016). When differentiated with BMP4 and bFGF, this difference in β-catenin expression was further accentuated (Fig. S7A-B). However, when β-catenin degradation was inhibited using the GSK3 inhibitor CHIR99201, the differences in β-catenin expression between the soft and hard regions, as well as the expression differences of T, were abolished (Fig. S7C-D). This suggests that spatially controlling of stem cell fate , by manipulating local stiffness likely involves a combined effect of YAP and Wnt/β-catenin signaling. In the hard region, nuclear-localized YAP and decreased β-catenin negatively affect Wnt signaling. In contrast, at soft region, decreased YAP nuclear trafficking and upregulated β-catenin enhance sensitivity to Wnt stimulation, resulting in spatially distinct cell fates (Fig. 6E).

Disscussion

We developed a photocurable hydrogel for hPSCs culture. We have also shown that spatial pattern illumination of UV light using a digital mirror device could control the shape of the gel pattern and the local stiffness. Laminin511 E8 fragment functionalized hydrogel supports hPSCs growth and maintained pluripotency. hPSCs can be differentiated towards all three germ layers on our developed hydrogel. We also demonstrated when cultured on the gel, β-Catenin formation, and endoderm related genes are upregulated compared to hard gels and PS dishes. Most importantly, by generating locally soft gels, we could selectively differentiate hPSCs towards the early mesoderm and manipulate stem cell fate spatially.

To overcome the limitation of traditional 2D/3D cultures, many soft substrates have been developed for cell cultures, such as various hydrogels, electro-spun fibers, and PDMS. However, due to the poor adhesivity of hPSCs on the synthetic surface (Tibbitt and Anseth, 2009; Virdi and Pethe, 2021), only limited materials can be used for attachment culture. PA has been used for hPSCs attachment culture; however, the pluripotency cannot be maintained. Here, Laminin 511 E8 was covalently bonded to our hydrogel and provided a strong attachment for hPSCs to enable an ideal culture of hPSCs while maintaining pluripotency.

Soft substrates such as PVA, electro-spun fibers, PA gel, and PDMS have previously been used for hPSCs attachment culture (Chen et al., 2020; Hsu et al., 2018; Keung et al., 2012; Kumbar et al., 2008; Muduli et al., 2017; Muncie et al., 2020; Musah et al., 2014; Pagliari et al., 2021; Przybyla et al., 2016; Virdi and Pethe, 2021). However, these methods usually coat the whole surface of the culture dish, and the local physical property cannot be adjusted. Recent research suggests the importance of the stiffness and geometry constraint in differentiating complex structures (Chen et al., 2020; Karzbrun et al., 2021; Keung et al., 2012; Martyn et al., 2018; Muncie et al., 2020; Musah et al., 2014; Przybyla et al., 2016; Rosowski et al., 2015; Srivastava et al., 2023; Virdi and Pethe, 2021). Our hydrogel provided

a simple and flexible platform for generating a geometry- and local stiffness-defined culture substrate.

Currently, most of the differentiation protocol was developed by adjusting the culture medium composition. However, organs are an organized structure of different lineages. Differentiation of different lineages in a homogenous culture system by only adjusting medium composition is challenging. Here, we selectively differentiate hPSCs towards the mesoderm by adjusting local stiffness; this provided a new tool for generating complex structures and contributing to regenerative medicine and tissue engineering.

The physical microenvironment plays a critical role in stem cell fate determination. We noticed that when differentiating hESCs on different stiffness substrates, the expression changes of marker genes do not appear linear with stiffness (Maldonado et al., 2017; Musah et al., 2014). It has been previously reported that in the range of 3 kPa to 1GPa, the expression of APS and mesendoderm genes (EOMES and Brachyury) and DE genes (FOXA2 and SOX17) is inversely proportional to the substrate stiffness, but a soft substrate seems to inhibit pan primitive streak gene, CDX2, and mesodermal genes, FOXC2 and NKX2.5(Chen et al., 2020). Substrate stiffness also affects the cell fate decision developmental stage specifically. PM-related genes remained at similar expression levels in our experiment could be explained by different observed markers, time points and stiffness range.

Furthermore, even for a similar stiffness range, studies using different materials, such as electrospun nanofibers, have different results from those using hydrogels (Chen et al., 2020; Maldonado et al., 2017; Przybyla et al., 2016), indicating the culture substrate might not only affect cells by mechanotransduction but also other factors such as the substrate dimensionality and surface chemistry. The type and distribution of ECM proteins have been shown to influence stem cell mechanosensation and fate in conjunction with substrate stiffness(Kechagia et al., 2023; Lee et al., 2019; Shibata et al., 2018; Stanton et al., 2019; Wang et al., 2015; Zhang et al., 2017). In our research, to provide stable cell attachment, we used a high density of laminin 511, known for its strong cell attachment properties. Previous reports have indicated that high density of ECM ligand on culture substrate promotes YAP nuclear trafficking. Our gel also exhibits a higher protein binding capacity compared to commercial glass dishes (Fig. 1G-H), resulting in a denser ligand density. This might explain why stem cells were able to exhibit nuclear-localized YAP even when cultured on our

relatively soft gel (700kPa~6kPa). The interplay between ECM proteins and stiffness warrants further examination in future research.

We also found that endoderm gene expression was promoted on our gel, as indicated by our RNA-seq results (Fig. S2), consistent with previous reports(Guo et al., 2020; Keung et al., 2012) Our developed hydrogel model promotes DE differentiation, likely through the upregulation of NODAL signaling mediated by LINC00458 and SMAD 2/3 upregulation as shown before(Guo et al., 2020; Keung et al., 2012).

The mechanism of how our hydrogel, with other substrates, affects stem cell behavior is an important aspect to explore. Most studies discussing substrate stiffness used hydrogels (Chen et al., 2020; Keung et al., 2012; Maldonado et al., 2017; Muduli et al., 2017; Muncie et al., 2020; Pagliari et al., 2021; Przybyla et al., 2016; Virdi and Pethe, 2021). hydrogels are polymer networks containing water molecules within these networks. Changing the number of cross-links also changes the mesh size and surface chemistry, thus affecting the diffusion of the soluble factors at the basal side of the cell. In our research, we have shown that our gel can only allow small soluble factors (1.4kDa) to penetrate but not those molecules that are bigger than 4kDa, suggesting that it is unlikely that the manipulation of stem cell fate in this study is caused by differences of diffusible proteins such as those of TGFβ.

We've shown YAP nuclear trafficking downregulation and β-catenin upregulation on softer gels. Our gel enables spatial manipulation of YAP and Wnt/β-catenin signaling for stem cell fate control in early mesoderm differentiation. Future research should explore the crosstalk between YAP and Wnt/β-catenin.

In summary, we have developed a novel method for the fabrication of hPSCs culture substrate. Taking advantage of the flexibility of gel geometry and stiffness, we could precisely control the geometry and spatial stiffness. By adjusting the stiffness locally, we could selectively differentiate hPSCs toward the mesoderm, providing a novel method to generate more complex tissue structures *in vitro*.

Methods

Synthesis and preparation of hydrogel prefabrication solution

PVA (AP-17, Japan Vinyl Acetate & Poval Co., Ltd. Mn= 80,000–90,000) was reconstituted into a 5% PVA solution by slowly adding PVA into 50–60℃ H_2O while stirring. The temperature was then increased to 90℃ while stirring for 60 min for PVA to completely dissolve. The solution was subsequently cooled to 50 ℃ while stirring. Sulfuric acid (400 µL) was added to the PVA solution dropwise while the temperature was maintained at approximately 50℃. Methacrylic anhydride (1.5 mL) (Catalog #276685, Sigma-Aldrich, St. Louis, United States) was added to the mixture dropwise while stirring until the mixture became cloudy. More sulfuric acid was added dropwise until the solution became clear. The temperature was maintained at approximately 50℃. The reaction proceeded with stirring at 50℃ overnight. The reaction product was transferred into a dialysis tube (Standard RC Tubing 6–8 kD Catalog #**15370752**, Spectrum Laboratories, Inc., Göteborg, Sweden) and dialyzed at 50℃ for 7–10 times. Obtained PVA-MA solution was then lyophilized to obtain PVA-MA powder. Prefabrication solution was prepared by reconstituting PEG, PVA-MA, and LAP in PBS to a final concentration of 10%, 5%, and 0.5% respectively. The solution was then adequate and stored in dark at -20℃. Prefabrication solution was hardened whether by using a patterned UV irradiation device or desktop UV stove in all experiments.

Activation of hydrogel and protein binding

The carboxyl groups of the prepared hydrogels were activated by incubating the hydrogel with 10 mg/ml each of NHS/EDC in MES solution at 37℃ for 2 h. The solution was replaced with Laminin 511 E8 fragment (Imatrix511, Catalog #T304, TAKARA BIO, Kusatsu, Japan) solution (30 µL in 1 mL of PBS) incubated at 37℃ overnight. The next day, the hydrogel was washed three times with PBS and used for cell culture following standard protocol.

Fluorescent Diffusion Test

Hydrogels were prepared as described previously. They were then incubated with solutions of fluorescent molecules in PBS for 8 hours. Cross sectional Z-stack photos of gels were

taken using a fluorescence inverted microscope (SP8 LIGHTNING Confocal Microscope, Leica, Wetzlar, Germany), and the fluorescence intensity was quantified using LAS X (V 1.4.5 27713, Leica, Wetzlar, Germany). Details regarding the fluorescent molecules used can be found in Table S3.

Cell culture

The human embryonic stem cell line, KhES-1, was used in this study. All cells used in this research are below passage number 50. KhES-1 was cultured at feeder-free conditions using StemFit® AK02N (Catalog #RCAK02N, TAKARA BIO, Kusatsu, Japan) with daily medium change. Cells were routinely passaged every week. On passage day, cells were washed in PBS twice and digested using 50% CTS™ TrypLE™ Select Enzyme (Thermo fisher, Catalog #A1285901) at 37°C for 5 min. CTS™ TrypLE™ Select Enzyme was then replaced with 2 mL PBS. Cells were collected by gently pipetting and centrifuging at 600g for 5 min. ROCK Inhibitor Y-27632 (Catalog #72302, STEMCELL Technologies, Vancouver, Canada) (10 M) was added during passage to improve survival and removed the next day. Laminin 511 E8 fragment (#T304, TAKARA BIO, Kusatsu, Japan) (2.5 µg/mL) was added into the medium during passage as the cell culture matrix.

Generation of H2B-mCherry cell line

PiggyBac donor vector containing H2B fusion mCherry-IRES-puromycin resistant gene under a CAG promoter, PB-CAG-H2B-mCherry-IPuroR is a kind gift from Dr.Ohgushi. pCMV-hyPBase is a kind gift from Dr. Yusa(Yusa et al., 2011). PB-CAG-H2B-mCherry-IPuroR and pCMV-hyPBase were co-transfected into KhES-1 using Fugene 6 (Promega, E269A) transfection reagent following the manufacturer's instruction. Three days after transfection, 1 µg/mL of puromycin was added to the culture medium to eradicate none integrated cells. Single colonies with a strong H2B-mCherry fluorescence signal were picked and expanded.

Generation of T-H2B-tdTomato Knock in cell line

T-2A-EGFP-PGK-Puro was a gift from James Thomson (Addgene plasmid # 83344; http://n2t.net/addgene:83344; RRID: Addgene_83344). T-2A-H2B-tdTomato was generated by replacing the EGFP fragment with H2B-tdTomato using the In-Fusion® HD Cloning Kit (Catalog #639648, Takara, Kusatsu, Japan), following the manufacturer's instructions, and then linearized using PCR.

A Cas9 and sgRNA all-in-one vector, containing the sgRNA sequence ACCTTCCATGTGAAGCAGCA targeting the 3' end of the T gene, was generated using the GeneArt® CRISPR Nuclease Vector Kit (Catalog #A21174, Thermo Fisher Scientific, Waltham, United States). The linear donor was then co-transfected with the Cas9 and sgRNA all-in-one vector into KhES-1 cells using the Neon™ Transfection System 100 µL Kit (Catalog #MPK10025, Thermo Fisher Scientific, Waltham, United States).

Three days after transfection, 1 µg/mL of puromycin was added to the culture medium to eliminate non-integrated cells. Single colonies were picked and expanded, and a stock was frozen at this stage. Colonies were then differentiated using 10 µM CHIR-99021(Catalog # 72052, STEMCELL Technologies, Vancouver, Canada) for 24 hours. Colonies showing co-expression of tdTomato and T were used for subsequent experiments.

Genomic PCR was employed to detect integration. The 3' and 5' junctions of the HDR site in integrated colonies were further confirmed by Sanger sequencing. The puromycin resistance cassette was subsequently removed from the genome by transfecting a vector containing CRE recombinase. A single colony with puromycin resistance was picked, expanded, and used for subsequent experiments. Oligonucleotides used can be found in Table S1

Interdivision time analysis

To compare the proliferation rate of cells cultured on gel and glass, soft or hard gel coated dish was generated following the previously described protocol. H2B-EGFP cells (1.5×10^5) were seeded into each dish and cultured following the standard protocol. Time-lapse was performed using Olympus LCV100 confocal live imaging system (Catalog # LCV100, Olympus, Tokyo, Japan) with an interval of 15 min/frame for 72 h. Cells (~100) inside similar size colonies on gel or glass from 3 dishes were manually tracked for interdivision time

analysis. The time between each nuclei division was measured according to 15 min/frame, the interdivision time of each cell was tracked at least three times and the mean value was recorded.

Cell culture on hydrogel

Glass bottom dishes (Catalog #3961-035, AGC TECHNO, Shizuoka, Japan) was coated using Bindsilane (Catalog # 10600047, GE Healthcare, Illinois, United States) following the manufacturer's instruction to improve hydrogel binding. Dishes were then coated with MPC polymer (Catalog # Lipidure-CM5206, NOR Corporation, Tokyo, Japan) to avoid attachment of cells on the none gel part of the dish following manufacturer instructions. The prefabrication solution was thawed and briefly vortexed. A prefabrication solution (20 µL) was added to one dish. Cover glass coated with Sigmacote® (Catalog # SL2-25ML, Sigma-Aldrich, St. Louis, United States) was gently put on the gel while avoiding generating bubbles to create a flat gel surface. The gel was then hardened using Desktop Maskless Lithography System (DDB-701-DL, NEOARK CORPORATION, Hachioji, Japan). For all experiments, hard gel was hardened with 100% output power UV for 10sec, and soft gel was hardened using 25% output power for 5sec. After gelation, the cover glass was gently removed, and then hydrogel was activated and functionalized using the Laminin511 E8 fragment. Cells were seeded following standard protocol. The culture medium was half replaced the next day of passage and were all replaced 2 days after passage to gradually remove Y-27632 to avoid detachment of cells. Cells were then maintained following a standard medium change schedule.

Stiffness Measurement of Hydrogels Using Atomic Force Microscope (AFM)

In this research, stiffness was exclusively represented by the elastic moduli. The Young's modulus of all hydrogels was measured using an AFM (NanoWizardIIR, BRUKER, Billerica, United States). To briefly explain, a tipless cantilever (TL-Cont) with a spring constant of 0.02 N/m and a 10 µm diameter bead attached to the tip were employed for subsequent measurements. These measurements were conducted in the Force Spectroscopy mode within a water medium. The elastic moduli presented here are Young's moduli, determined

by applying the Hertz model to force curves. Specifically, only the initial 500 nm of indentation was considered for fitting the force curves. After noise removal using NanoWizard software (V7, BRUKER, Billerica, United States), Young's modulus was calculated and analyzed with JPKSPM Data Processing software (V 4.2.1, JPK Instruments AG, Berlin, Germany).

Micropatterned culture on gel

In patterning culture, cells should be seeded at high density since they are cultured on top of the hydrogel patterns. Therefore, the cell seeding area was limited using a PDMS spacer. First, PDMS sheets were prepared by mixing the main agent: hardener = 9:1 for 15 min, and then pour onto a flat surface and cured by heating at 80°C for 15–20 min. The sheet was made as thin as possible for subsequent patterning culture. A hole of 6 mm diameter was made in the center of the formed PDMS sheet using a hole punch. PDMS spacer was attached to Bindsilane coated 35 mm glass-bottom dish and 20 µL of PVA-PEG prefabrication solution was added into the hole. Then Sigmacote® coated coverslip was gently put on top of the gel solution. The patterned gel was then cured by irradiating patterned UV using Desktop Maskless Lithography System (DDB-701-DL, NEOARK CORPORATION, Hachioji, Japan). Gel with different stiffness was generated by giving spatially different UV exposure (100% output for 10 seconds for the hard part and 25% output for 5 seconds for the soft part). Then coverslip was removed, and hydrogel was activated and functionalized with Laminin511 E8 fragment. hESCs (KhES-1) (1×10^6) were collected and resuspended in 200 µL of AK02N medium with 10 µM Y27632.The suspension (20 L) was added on top of the gel pattern and incubated at 37 °C, 5% CO_2 for 30 min to allow cells to attach. The gel was washed with PBS once to remove exceeded cells and the PDMS spacer was removed. AK02N medium (1 mL) with 10uM Y27632 was added to the dish. Half of the medium was replaced with AK02N the next day. Then Cells were cultured following standard protocol.

Mesoderm differentiation

Mesoderm differentiation was done following previously reported method(Evseenko et al., 2010). Shortly, hESCs cultured on gel pattern was generated following protocol

mentioned above. Cell culture medium was replaced with Stemline II Hematopoietic Stem Cell Expansion Medium(Catalog # S0192-500ML, Sigma-Aldrich, St. Louis, United States) or AK02N(for pulse differentiation) supplemented with 10ng each of BMP4(Catalog # H4916, Sigma-Aldrich, Tokyo, Japan) and bFGF(Catalog # 100-18B-1MG, Thermo Fisher Scientific, Waltham, USA) for 24hrs.

Live imaging of T-H2B-tdTomato

We generated a patterned culture on a gel with an oval shape, where half of it was soft, and the other half was hard, as previously described. In brief, T-H2B-tdTomato cells cultured on the gel pattern, which had locally different stiffness, were subjected to differentiation using either 10μM CHIR or 10ng/ml each of BMP4 and bFGF for 24 hours. Subsequently, the differentiating medium was removed, and the sample were washed twice with PBS before being returned to the maintenance culture medium.

For time-lapse recording of T expression, we utilized the Olympus LCV100 confocal live imaging system, capturing images at intervals of 60 minutes per frame for a duration of 48 hours.

Measuring protein binding ability of PVA-MA

PVA-MA hydrogel was prepared and activated as described previously. The hydrogel was then incubated with a fluorescent 2nd antibody (Catalog # A-11003, ThermoFisher, Massachusetts, United States) following the protein binding protocol described previously. Z stack Photos of the gel surface were taken using a fluorescence inverted microscope (SP8 LIGHTNING Confocal Microscope, Leica, Wetzlar, Germany) and the fluorescence intensity was quantified using LAS X(V 1.4.5 27713, Leica, Wetzlar, Germany).

Immunofluorescence

The culture medium was removed from the sample. Samples were then fixed by incubating in 2 mL of 4% PFA in PBS on ice for 20 min. the sample was washed in PBS, three times for 5 min each. PBS was replaced with 0.3% Triton-X100/PBS and samples were incubated for 5 min at 25℃. Samples were then blocked with Blocking One (Catalog #03953-66, NACALAI

TESQUE, Kyoto, Japan) for 1 h at room temperature, then incubated with primary antibody diluted in blocking one at 4°C overnight. primary antibody was Removed then samples were washed with 0.05% Tween 20/PBS for 5 min and repeated three times. Then samples were incubated with secondary antibodies and DAPI diluted in the blocking solution, 1/500 for 1 h at room temperature. Secondary antibodies were removed, and samples were washed in 0.05% Tween 20/PBS for 5 min, thrice. The samples were then observed using a microscope.

RNA extraction and quantitative PCR

Total RNA was extracted using RNeasy Mini Kit (Catalog #74106, QIAGEN, Hilden, Germany) following the manufacturer's instructions. cDNA was reverse transcripted from 500ng RNA using PrimeScript™ II 1st strand cDNA Synthesis Kit (Catalog # 6210A TAKARA BIO, Kusatsu, Japan) following the manufacturer's instructions. qPCR was performed using Power™ SYBR™ Green Master Mix (Catalog #4368577, Applied Biosystems™, Massachusetts, United States). The expression level of mRNAs was calculated and normalized based on indicated housekeeping gene (*HPRT1*, *PBGD*).

RNA-seq

Gel-coated 35 mm glass-bottom dishes were prepared as previously described. KhES-1 was seeded on the soft gel, hard gel, or uncoated glass-bottom dish and cultured for 4 days before they were collected as previously described. Total RNA was extracted using RNeasy Mini Kit (Cat#74106, QIAGEN, HILDEN, GERMANY,) following the manufacturer's instruction. Two samples for each group, 12 samples in total were collected. Libraries were prepared from 100 ng of total RNA using the following kits, NEBNext Poly(A) mRNA Magnetic Isolation Module (Catalog # E7490, NEW ENGLAND BIOLABS, MASSACHUSETTS, UNITED STATES), NEBNext Ultra II Directional RNA Library Prep Kit (Catalog # E7760, NEW ENGLAND BIOLABS,MASSACHUSETTS, UNITED STATES), NEBNext Multiplex Oligos for Illumina (96 Unique Dual Index Primer Pairs) (Catalog # E6440, NEW ENGLAND BIOLABS,MASSACHUSETTS, UNITED STATES) following the manufacturer's instructions. Sequencing was performed with the paired-end mode (more than 50 bp at both ends) to have at least 15 clusters per sample using the NextSeq550 NGS system. The generated raw RNA-seq files were quality trimmed with Trimomatic-0.39 and removed rRNA with bowtie2.

This highly qualified sequence reads were mapped and annotated with STAR-2.7.6a against the GRCh38, and then the count data which was estimated with featureCounts was subjected to differential expressed gene analysis using the bioconductor package DESeq2_1.30.1. The DEGs were defined as genes that were expressed with a false discovery rate < 0.01. Metascape database platform was used to enrich and analyze the GO (Gene ontology) annotation.

YAP quantification

Nucleocytoplasmic transport of YAP was quantified using the N/C intensity ratio (Kelley and Paschal, 2019) .In brief, cells cultured on hard and soft gels or on a rigid dish were subjected to immunofluorescence (IF) staining following the previously mentioned protocol. Z-stack images were acquired, and a Z-projection was generated using the Sum Slices method in ImageJ2(Rueden et al., 2017). To mitigate the impact of confluency on YAP localization, we focused on quantifying small colonies containing fewer than 20 cells.

To outline the process briefly, a DAPI image for nuclear staining was thresholded to create a mask that defines the nuclear area. The YAP-stained channel was also thresholded to delineate the cytoplasmic area containing the nuclear region. The nuclear area was then subtracted from the YAP-stained image using the mask generated from DAPI. The remaining area was used to measure the average fluorescence intensity of the cytoplasm. The N/C ratio was calculated as follows: N/C = Average intensity of the nucleus / Average intensity of the cytoplasm.

Statistical analysis

Statistical analysis was done using GraphPad Prism (V 9.3.1, GraphPad Software, La Jolla, United States). Two tail unpaired t test was used to compare the differences of each group.

Manuscript preparation

Manuscript was first written by the first author, ChatGPT (V 3.5, Open AI, San Francisco, US) was used to check and improve the clarity and grammar of written manuscript.

References

Candiello, J., Singh, S. S., Task, K., Kumta, P. N. and Banerjee, I. (2013). Early differentiation patterning of mouse embryonic stem cells in response to variations in alginate substrate stiffness. *J Biol Eng* **7**, 9.

Chambers, S. M., Fasano, C. A., Papapetrou, E. P., Tomishima, M., Sadelain, M. and Studer, L. (2009). Highly efficient neural conversion of human ES and iPS cells by dual inhibition of SMAD signaling. *Nat Biotechnol* **27**, 275-280.

Chen, G., Tang, W., Wang, X., Zhao, X., Chen, C. and Zhu, Z. (2019). Applications of Hydrogels with Special Physical Properties in Biomedicine. *Polymers (Basel)* **11**.

Chen, Y. F., Li, Y. J., Chou, C. H., Chiew, M. Y., Huang, H. D., Ho, J. H., Chien, S. and Lee, O. K. (2020). Control of matrix stiffness promotes endodermal lineage specification by regulating SMAD2/3 via lncRNA LINC00458. *Sci Adv* **6**, eaay0264.

D'Amour, K. A., Agulnick, A. D., Eliazer, S., Kelly, O. G., Kroon, E. and Baetge, E. E. (2005). Efficient differentiation of human embryonic stem cells to definitive endoderm. *Nat Biotechnol* **23**, 1534-1541.

Estaras, C., Hsu, H. T., Huang, L. and Jones, K. A. (2017). YAP repression of the WNT3 gene controls hESC differentiation along the cardiac mesoderm lineage. *Genes Dev* **31**, 2250-2263.

Evseenko, D., Zhu, Y., Schenke-Layland, K., Kuo, J., Latour, B., Ge, S., Scholes, J., Dravid, G., Li, X., MacLellan, W. R., et al. (2010). Mapping the first stages of mesoderm commitment during differentiation of human embryonic stem cells. *Proc Natl Acad Sci U S A* **107**, 13742-13747.

Gattazzo, F., Urciuolo, A. and Bonaldo, P. (2014). Extracellular matrix: a dynamic microenvironment for stem cell niche. *Biochim Biophys Acta* **1840**, 2506-2519.

Guo, A., Wang, B., Lyu, C., Li, W., Wu, Y., Zhu, L., Bi, R., Huang, C., Li, J. J. and Du, Y. (2020). Consistent apparent Young's modulus of human embryonic stem cells and derived cell types stabilized by substrate stiffness regulation promotes lineage specificity maintenance. *Cell Regeneration* **9**.

Hsu, H.-T., Estarás, C., Huang, L. and Jones, K. A. (2018). Specifying the anterior primitive streak by modulating YAP1 levels in human pluripotent stem cells. *Stem cell reports* **11**, 1357-1364.

Karzbrun, E., Khankhel, A. H., Megale, H. C., Glasauer, S. M. K., Wyle, Y., Britton, G., Warmflash, A., Kosik, K. S., Siggia, E. D., Shraiman, B. I., et al. (2021). Human neural tube morphogenesis in vitro by geometric constraints. *Nature* **599**, 268-272.

Kechagia, Z., Saez, P., Gomez-Gonzalez, M., Canales, B., Viswanadha, S., Zamarbide, M., Andreu, I., Koorman, T., Beedle, A. E. M., Elosegui-Artola, A., et al. (2023). The laminin-keratin link shields the nucleus from mechanical deformation and signalling. *Nat Mater*.

Kelley, J. B. and Paschal, B. M. (2019). Fluorescence-based quantification of nucleocytoplasmic transport. *Methods* **157**, 106-114.

Keung, A. J., Asuri, P., Kumar, S. and Schaffer, D. V. (2012). Soft microenvironments promote the early neurogenic differentiation but not self-renewal of human pluripotent stem cells. *Integrative Biology* **4**, 1049-1058.

Kumbar, S. G., James, R., Nukavarapu, S. P. and Laurencin, C. T. (2008). Electrospun nanofiber scaffolds: engineering soft tissues. *Biomed Mater* **3**, 034002.

Lee, S., Stanton, A. E., Tong, X. and Yang, F. (2019). Hydrogels with enhanced protein conjugation efficiency reveal stiffness-induced YAP localization in stem cells depends on biochemical cues. *Biomaterials* **202**, 26-34.

Lee, S., Tong, X. and Yang, F. (2014). The effects of varying poly(ethylene glycol) hydrogel crosslinking density and the crosslinking mechanism on protein accumulation in three-dimensional hydrogels. *Acta Biomater* **10**, 4167-4174.

Loh, K. M., Ang, L. T., Zhang, J., Kumar, V., Ang, J., Auyeong, J. Q., Lee, K. L., Choo, S. H., Lim, C. Y., Nichane, M., et al. (2014). Efficient endoderm induction from human pluripotent stem cells by logically directing signals controlling lineage bifurcations. *Cell Stem Cell* **14**, 237-252.

Loh, K. M., Chen, A., Koh, P. W., Deng, T. Z., Sinha, R., Tsai, J. M., Barkal, A. A., Shen, K. Y., Jain, R., Morganti, R. M., et al. (2016). Mapping the Pairwise Choices Leading from Pluripotency to Human Bone, Heart, and Other Mesoderm Cell Types. *Cell* **166**, 451-467.

Maldonado, M., Luu, R. J., Ico, G., Ospina, A., Myung, D., Shih, H. P. and Nam, J. (2017). Lineage- and developmental stage-specific mechanomodulation of induced pluripotent stem cell differentiation. *Stem Cell Res Ther* **8**, 216.

Martyn, I., Brivanlou, A. H. and Siggia, E. D. (2019). A wave of WNT signaling balanced by secreted inhibitors controls primitive streak formation in micropattern colonies of human embryonic stem cells. *Development* **146**, dev172791.

Martyn, I., Kanno, T. Y., Ruzo, A., Siggia, E. D. and Brivanlou, A. H. (2018). Self-organization of a human organizer by combined Wnt and Nodal signalling. *Nature* **558**, 132-135.

Millar-Haskell, C. S., Dang, A. M. and Gleghorn, J. P. (2019). Coupling synthetic biology and programmable materials to construct complex tissue ecosystems. *MRS Commun* **9**, 421-432.

Muduli, S., Chen, L. H., Li, M. P., Heish, Z. W., Liu, C. H., Kumar, S., Alarfaj, A. A., Munusamy, M. A., Benelli, G., Murugan, K., et al. (2017). Stem cell culture on polyvinyl alcohol hydrogels having different elasticity and immobilized with ECM-derived oligopeptides. *J Polym Eng* **37**, 647-660.

Muncie, J. M., Ayad, N. M. E., Lakins, J. N., Xue, X., Fu, J. and Weaver, V. M. (2020). Mechanical Tension Promotes Formation of Gastrulation-like Nodes and Patterns Mesoderm Specification in Human Embryonic Stem Cells. *Dev Cell* **55**, 679-694 e611.

Musah, S., Wrighton, P. J., Zaltsman, Y., Zhong, X., Zorn, S., Parlato, M. B., Hsiao, C., Palecek, S. P., Chang, Q., Murphy, W. L., et al. (2014). Substratum-induced differentiation of human pluripotent stem cells reveals the coactivator YAP is a potent regulator of neuronal specification. *Proceedings of the National Academy of Sciences* **111**, 13805-13810.

Pagliari, S., Vinarsky, V., Martino, F., Perestrelo, A. R., Oliver De La Cruz, J., Caluori, G., Vrbsky, J., Mozetic, P., Pompeiano, A., Zancla, A., et al. (2021). YAP–TEAD1 control of cytoskeleton dynamics and intracellular tension guides human pluripotent stem cell mesoderm specification. *Cell Death & Differentiation* **28**, 1193-1207.

Perez-Puyana, V., Jimenez-Rosado, M., Romero, A. and Guerrero, A. (2020). Polymer-Based Scaffolds for Soft-Tissue Engineering. *Polymers (Basel)* **12**.

Przybyla, L., Lakins, J. N. and Weaver, V. M. (2016). Tissue Mechanics Orchestrate Wnt-Dependent Human Embryonic Stem Cell Differentiation. *Cell Stem Cell* **19**, 462-475.

Qin, H., Hejna, M., Liu, Y., Percharde, M., Wossidlo, M., Blouin, L., Durruthy-Durruthy, J., Wong, P., Qi, Z., Yu, J., et al. (2016). YAP Induces Human Naive Pluripotency. *Cell Rep* **14**, 2301-2312.

Rosowski, K. A., Mertz, A. F., Norcross, S., Dufresne, E. R. and Horsley, V. (2015). Edges of human embryonic stem cell colonies display distinct mechanical properties and differentiation potential. *Sci Rep* **5**, 14218.

Rueden, C. T., Schindelin, J., Hiner, M. C., DeZonia, B. E., Walter, A. E., Arena, E. T. and Eliceiri, K. W. (2017). ImageJ2: ImageJ for the next generation of scientific image data. *BMC Bioinformatics* **18**, 529.

Shao, Y., Sang, J. and Fu, J. (2015). On human pluripotent stem cell control: The rise of 3D bioengineering and mechanobiology. *Biomaterials* **52**, 26-43.

Shibata, S., Hayashi, R., Okubo, T., Kudo, Y., Katayama, T., Ishikawa, Y., Toga, J., Yagi, E., Honma, Y., Quantock, A. J., et al. (2018). Selective Laminin-Directed Differentiation of Human Induced Pluripotent Stem Cells into Distinct Ocular Lineages. *Cell Rep* **25**, 1668-1679 e1665.

Simunovic, M. and Brivanlou, A. H. (2017). Embryoids, organoids and gastruloids: new approaches to understanding embryogenesis. *Development* **144**, 976-985.

Srivastava, P., Romanazzo, S., Kopecky, C., Nemec, S., Ireland, J., Molley, T. G., Lin, K., Jayathilaka, P. B., Pandzic, E., Yeola, A., et al. (2023). Defined Microenvironments Trigger In Vitro Gastrulation in Human Pluripotent Stem Cells. *Adv Sci* **10**.

Stanton, A. E., Tong, X., Lee, S. and Yang, F. (2019). Biochemical Ligand Density Regulates Yes-Associated Protein Translocation in Stem Cells through Cytoskeletal Tension and Integrins. *ACS Appl Mater Interfaces* **11**, 8849-8857.

Stronati, E., Giraldez, S., Huang, L., Abraham, E., McGuire, G. R., Hsu, H. T., Jones, K. A. and Estaras, C. (2022). YAP1 regulates the self-organized fate patterning of hESC-derived gastruloids. *Stem Cell Reports* **17**, 211-220.

Surmacz, B., Fox, H., Gutteridge, A., Fish, P., Lubitz, S. and Whiting, P. (2012). Directing differentiation of human embryonic stem cells toward anterior neural ectoderm using small molecules. *Stem Cells* **30**, 1875-1884.

Tibbitt, M. W. and Anseth, K. S. (2009). Hydrogels as extracellular matrix mimics for 3D cell culture. *Biotechnol Bioeng* **103**, 655-663.

Virdi, J. K. and Pethe, P. (2021). Biomaterials regulate mechanosensors YAP/TAZ in stem cell growth and differentiation. *Tissue Engineering and Regenerative Medicine* **18**, 199-215.

Wang, H., Luo, X. and Leighton, J. (2015). Extracellular Matrix and Integrins in Embryonic Stem Cell Differentiation. *Biochem Insights* **8**, 15-21.

Warmflash, A., Sorre, B., Etoc, F., Siggia, E. D. and Brivanlou, A. H. (2014). A method to recapitulate early embryonic spatial patterning in human embryonic stem cells. *Nat Methods* **11**, 847-854.

Yusa, K., Zhou, L. Q., Li, M. A., Bradley, A. and Craig, N. L. (2011). A hyperactive piggyBac transposase for mammalian applications. *P Natl Acad Sci USA* **108**, 1531-1536.

Zhang, D. W., Yang, S. Z., Toledo, E. M., Gyllborg, D., Salto, C., Villaescusa, J. C. and Arenas, E. (2017). Niche-derived laminin-511 promotes midbrain dopaminergic neuron survival and differentiation through YAP. *Science Signaling* **10**.

Acknowledgments

We appreciate the Single-Cell Genome Information Analysis Core (SignAC) at WPI-ASHBi, Kyoto University, for RNA-sequencing; K. Yusa for the PiggyBac vector. This work was supported by Core Research for Evolutional Science and Technology (CREST) by JST (JPMJCR12W2 to M.E.), JST SPRING (Grant Number JPMJSP2110 to Z.W.), Grant-in-Aid for JSPS Research Fellow (Grant Number 22J10657 to Z.W.).

Author contributions

Z.W., A.N., and M.E. designed the research; Z.W. and A.N. performed the research; Z.W., A.N., F.W., and Y.O. analyzed the data. Z.W. and M.E wrote the paper.

Data availability statement

The data and materials supporting this research are available from the authors on reasonable request. RNA-seq data has been deposited in the SRA database and may be accessed with the accession number PRJNA1022777

Additional information

The authors declare no competing interests.

Figure legends

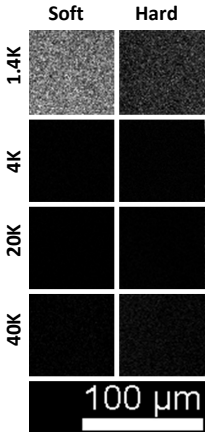

Fig. S1: Fluorescent Diffusion Experiment
Hydrogels were incubated with fluorescent molecules and then observed using laser confocal microscopy to assess the diffusion of fluorescent molecules inside the gel.
Scale bars: 100 µm.

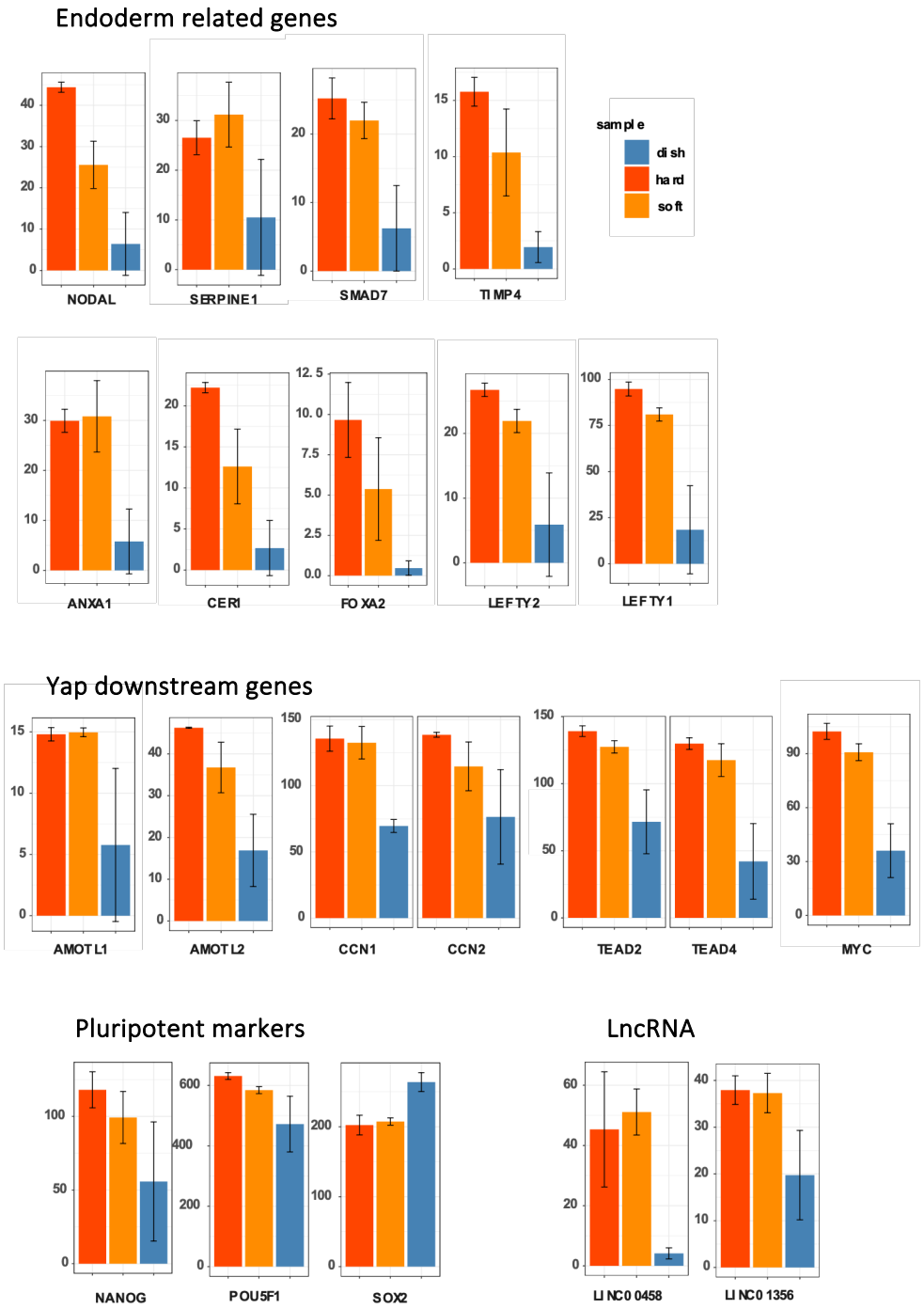

Fig. S2: Selected Gene Expression Based on RNA-seq
Expression levels of selected genes based on RNA-seq of hPSCs cultured on soft/hard gel and dish. Expression level is shown as TPM (Transcripts Per Kilobase Million).

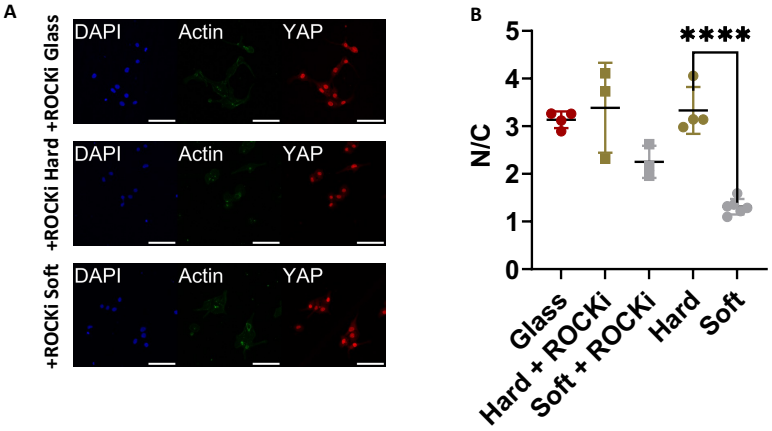

Figure S3: Immunofluorescent (IF) Staining and YAP Quantification (A) IF Staining of YAP: Immunofluorescent staining of YAP in cells cultured on soft/hard gel or glass with 10µM Y-27632. Scale bars: 100 µm. **(B) Quantification of YAP Nuclear Localization:** Quantification of YAP nuclear localization by Nuclear/Cytoplasmic fluorescent intensity ratio (N/C). Each dot represents individual quantification. Black lines represent median values. Error bars represent standard deviation. **** $P < 0.0001$ (unpaired, two-tailed t-test).

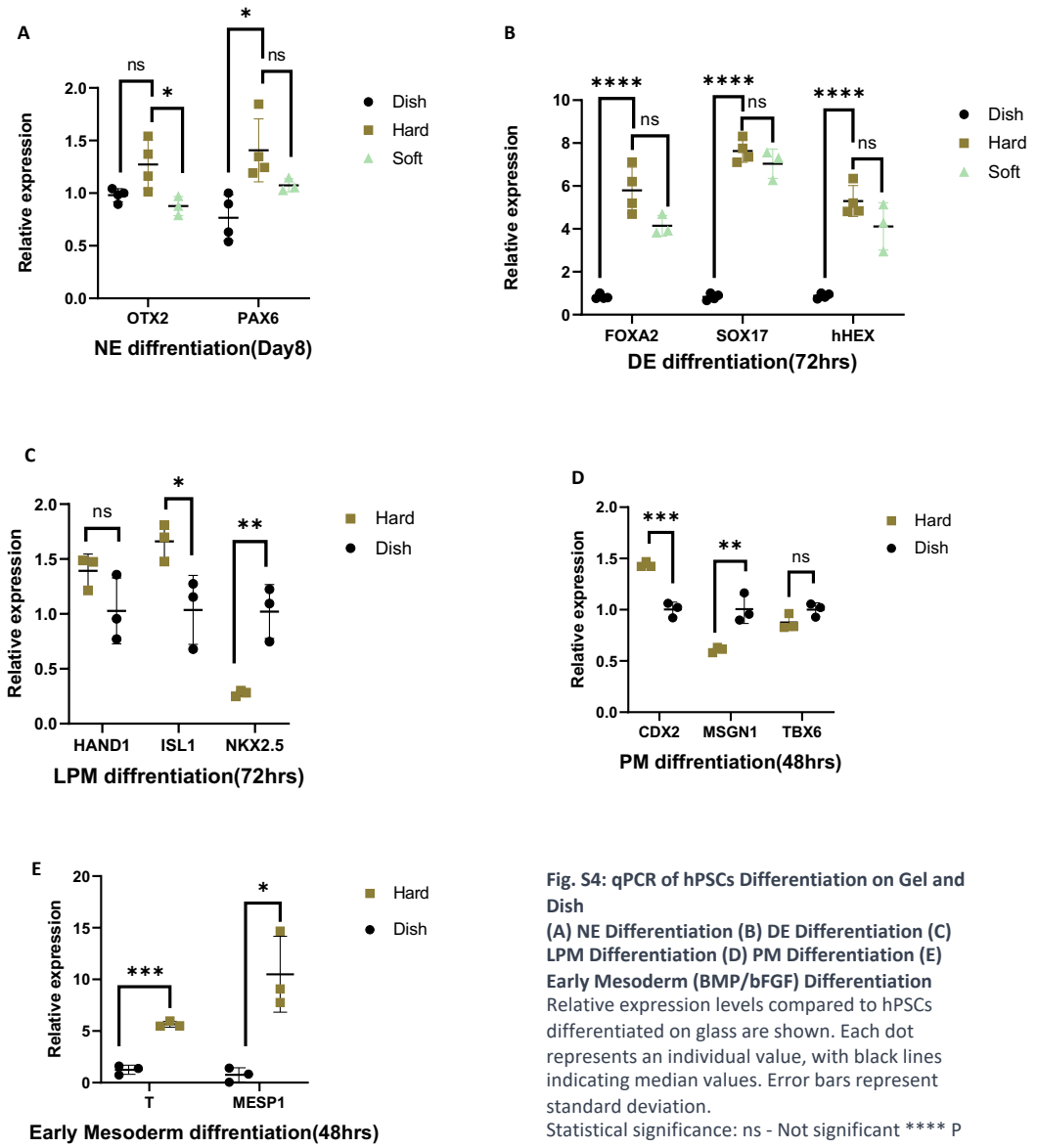

Fig. S4: qPCR of hPSCs Differentiation on Gel and Dish
(A) NE Differentiation (B) DE Differentiation (C) LPM Differentiation (D) PM Differentiation (E) Early Mesoderm (BMP/bFGF) Differentiation
Relative expression levels compared to hPSCs differentiated on glass are shown. Each dot represents an individual value, with black lines indicating median values. Error bars represent standard deviation.
Statistical significance: ns - Not significant **** P < 0.0001 *** P < 0.001 ** P < 0.01 *P < 0.1 (unpaired, two-tailed t-test).

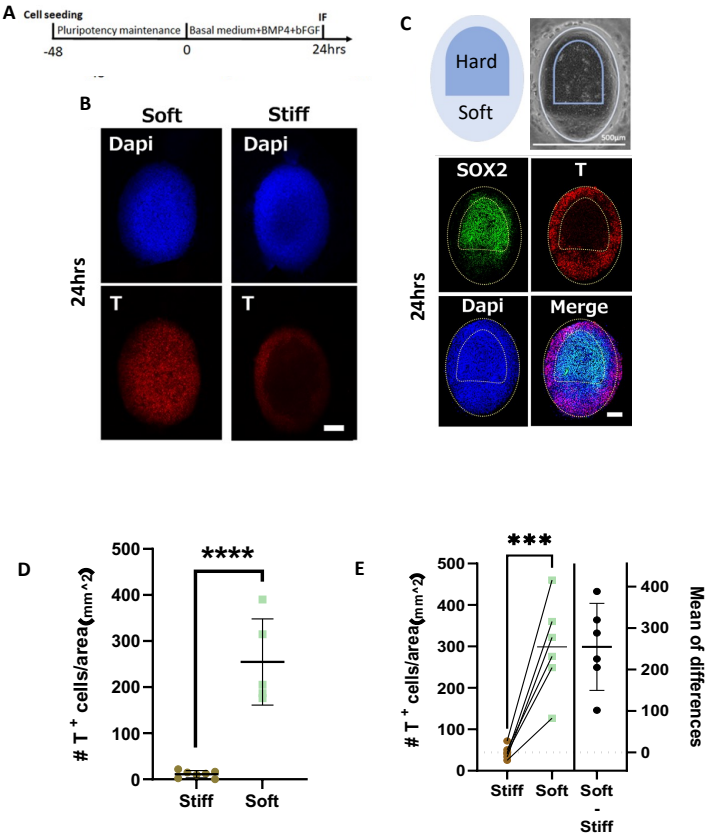

Fig. S5: Manipulating Stem Cell Fate by Adjusting Local Stiffness of the Hydrogel

(A) Differentiation Timetable for Mesoderm Differentiation (B) Immunofluorescence (IF) of 24-hour Mesoderm Differentiation on Soft and Hard Gels Scale bars: 100 µm. **(C) IF of 24-hour Mesoderm Differentiation on Gel with Locally Different Stiffness** Scale bars: 500 µm in bright filde,100 µm in IF image. **(D) Quantification of T+ Number/Area on Soft and Hard Gels (n=5) (E) Quantification of T+ Number/Area on Each Gel with Locally Different Stiffness (n=6).** Each dot represents an individual value, with black lines indicating median values. Error bars represent standard deviation. Statistical significance: **** $P < 0.0001$ *** $P < 0.001$ (unpaired, two-tailed t-test).

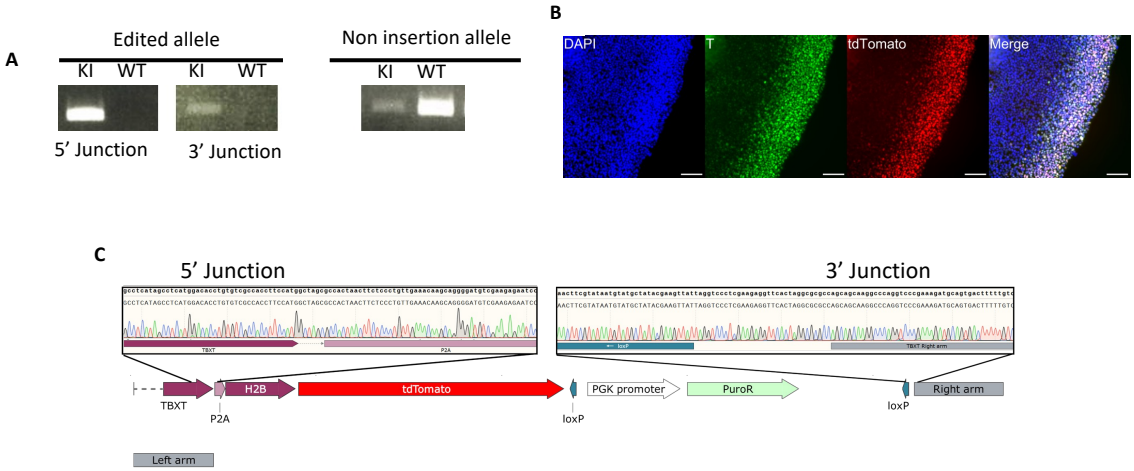

Fig. S6: Verification of Knock-in Reporter T-H2B-tdTomato (A) Genomic PCR of T-H2B-tdTomato: Electrophoresis showing successful heterogeneous integration into the genome. **(B) Immunofluorescence (IF) of T-H2B-tdTomato:** Differentiated with 10µM CHIR for 24 hours, showing colocalization of tdTomato and T expression. Scale bars: 100 µm.
(C) Sanger Sequencing of Junction of Integrated Fragment

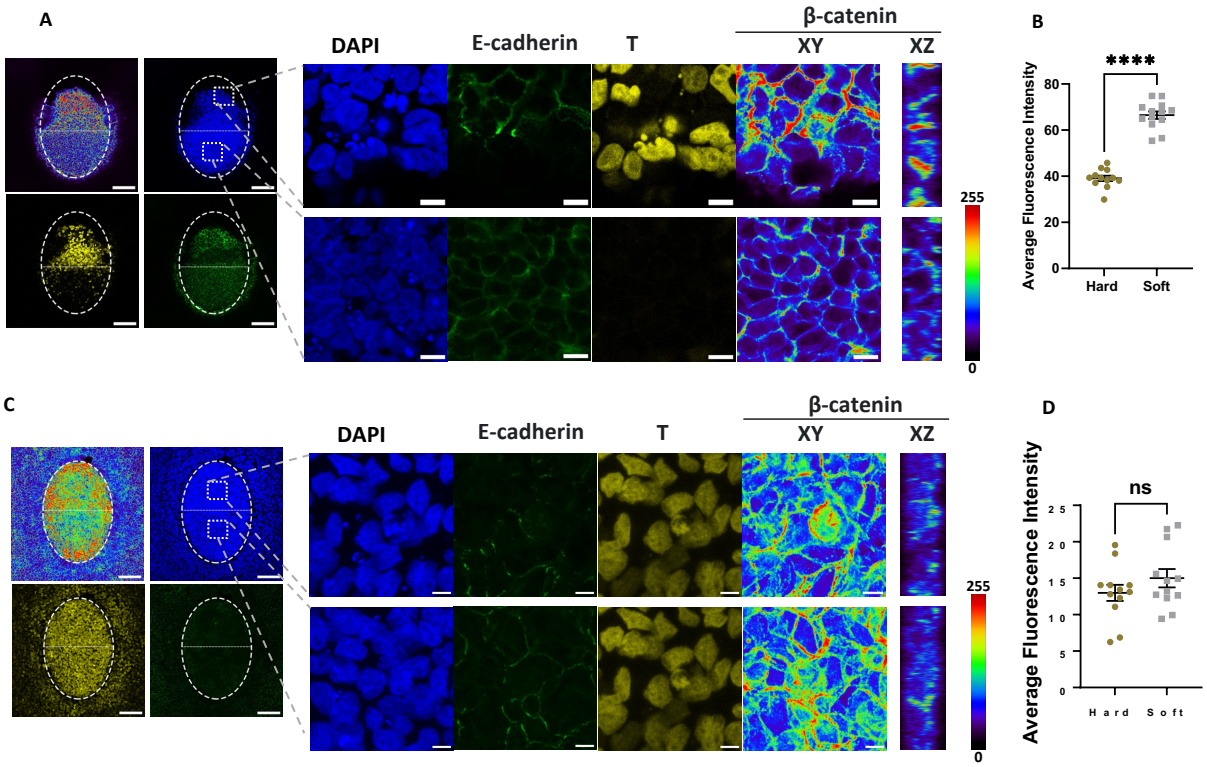

Fig. S7: Stem Cell Fate Control Can Be Achieved with BMP/bFGF but Not CHIR (A) IF Staining (Differentiated with BMP/bFGF): Immunofluorescent staining of hPSCs on a partially soft gel pattern using pulsed differentiation, as shown in Fig. 5C. The white dotted oval line indicates the entire gel pattern, with the upper half being soft and the lower half being hard. The white box indicates a magnified view of the indicated region. The β-catenin channel is shown in XY and XZ section views as a heat map, with colors representing fluorescent intensity. Scale bars: 100 µm in the whole gel view and 10 µm in the magnified view. **(B) Quantification of β-catenin in BMP/bFGF Differentiation:** Quantification of β-catenin fluorescent intensity based on Z sections of IF staining in BMP/bFGF differentiation on a partially soft gel. **(C) IF Staining (Differentiated with CHIR):** Immunofluorescent staining of hPSCs on a partially soft gel pattern using pulsed differentiation with CHIR. The white dotted oval line indicates the entire gel pattern, with the upper half being soft and the lower half being hard. The white box indicates a magnified view of the indicated region. The β-catenin channel is shown in XY and XZ section views as a heat map, with colors representing fluorescent intensity. Scale bars: 100 µm in the whole gel view and 10 µm in the magnified view. **(D) Quantification of β-catenin in CHIR Differentiation:** Quantification of β-catenin fluorescent intensity based on Z sections of IF staining in CHIR differentiation on a partially soft gel. Each dot represents an individual measurement. The black line represents the mean value. Statistical significance: ns - Not significant **** $P < 0.0001$ (unpaired, two-tailed t-test). Error bars represent standard deviation.

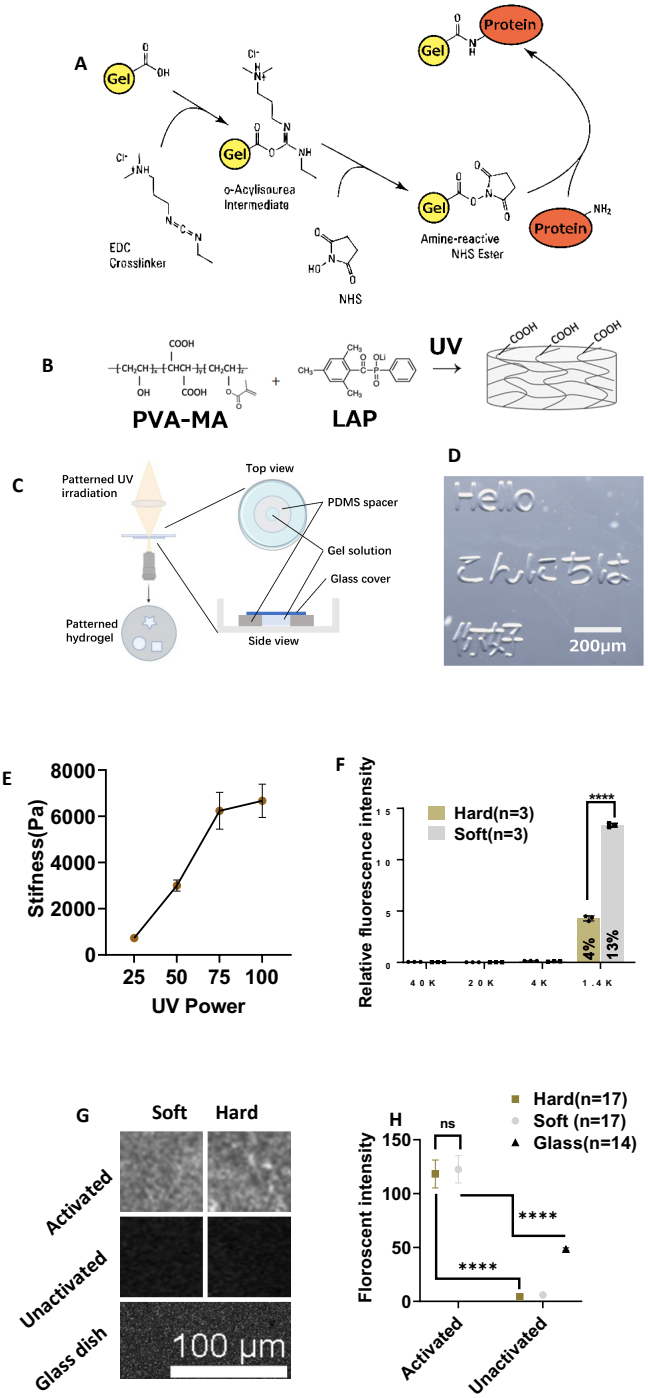

Fig. 1: Photocurable PVA-PEG Hydrogel (A) Schematic Illustration: The hydrogel can be activated to bond with proteins using NHS/EDC.**(B) Illustration:** PVA-MA forms COOH-containing hydrogel upon ultraviolet (UV) irradiation.**(C) Schematic Illustration:** Generating patterned hydrogel.**(D) Patterned Gel Generation:** Patterned gel was generated using patterned UV irradiation as shown in Figure 1C.**(E) Stiffness Measurement:** Stiffness measured for hydrogel generated using different UV dosages. Dots represent mean values; n=20.**(F) Fluorescent Diffusion Experiment:** Hydrogels were incubated with fluorescent molecules. Bars show the mean value of fluorescent intensity inside the gel relative to incubation solution. Black dots represent each sample.**(G) Pictures of Fluorescent Protein Binding Experiments:** Activated and non-activated soft/hard gels, together with a glass-bottom dish, were incubated with fluorescent protein to evaluate the protein binding ability.**(H) Quantification of Fluorescent Protein Binding Experiments:** Fluorescent intensity was measured using fluorescent microscopy. Legends represent the mean value of each group.

Scale bars: 200 μm in D, 100 μm in G. Black lines represent median values. ns Not significant. **** $P < 0.0001$(unpaired, two-tailed t-test). Error bars represent standard deviation.

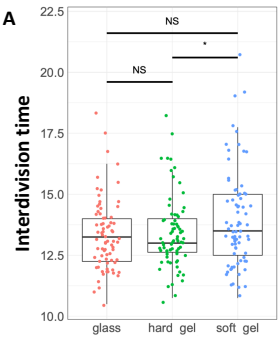

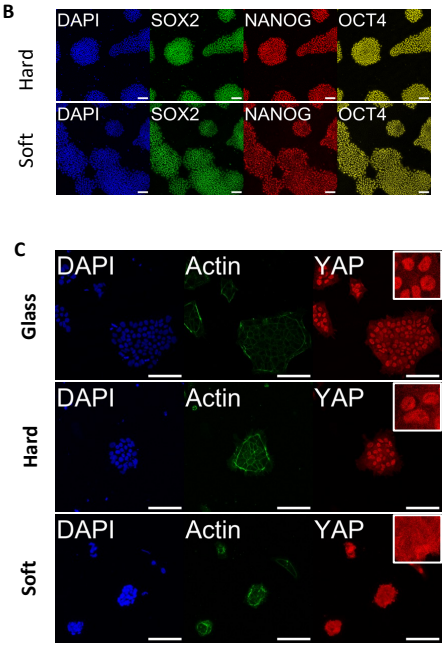

Fig. 2: Human Pluripotent Stem Cells (hPSCs) Proliferation and YAP Localization(A) Interdivision Time: Interdivision time of hPSCs cultured on hard gel, soft gel, and conventional culture dishes. Dots represent individual cells.**(B) Pluripotent Marker Staining:** Immunofluorescent (IF) staining of pluripotent markers in day 6 cells cultured on soft and hard gels.**(C) YAP Staining:** IF staining of YAP in hPSCs cultured on gels and conventional dishes. White boxes indicate 40×40 μm area magnifications of YAP staining. Scale bar: 100 μm. NS Not significant. * $P < 0.1$(unpaired, two-tailed t-test). Error bars represent standard deviation.

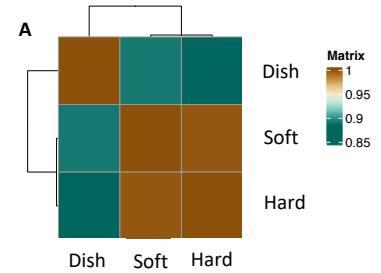

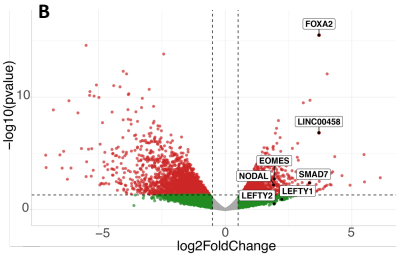

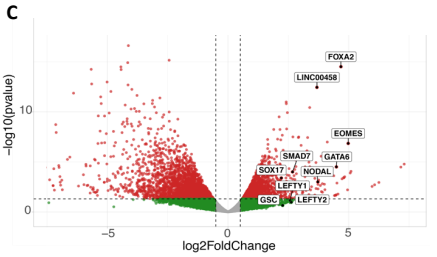

D

R-HSA-201722: Formation of the beta-catenin:TCF transactivating complex
GO:0032328: alanine transport
GO:0061061: muscle structure development
GO:0000902: cell morphogenesis
GO:0007492: endoderm development
GO:0120035: regulation of plasma membrane bounded cell projection organization
GO:0022604: regulation of cell morphogenesis
WP3651: Pathways affected in adenoid cystic carcinoma
GO:1903510: mucopolysaccharide metabolic process
WP5087: Malignant pleural mesothelioma
GO:0042254: ribosome biogenesis
WP4718: Cholesterol metabolism with Bloch and Kandutsch-Russell pathways
GO:0051568: histone H3-K4 methylation
GO:0001570: vasculogenesis
GO:0042698: ovulation cycle
GO:0007157: heterophilic cell-cell adhesion via plasma membrane cell adhesion molecules
GO:0000165: MAPK cascade
R-HSA-1474228: Degradation of the extracellular matrix
GO:0001822: kidney development
GO:0030240: skeletal muscle thin filament assembly

Top 20 enriched GO term of soft gel

E

GO:0022613: ribonucleoprotein complex biogenesis
R-HSA-212165: Epigenetic regulation of gene expression
GO:0006338: chromatin remodeling
GO:0007507: heart development
GO:0043414: macromolecule methylation
GO:0009792: embryo development ending in birth or egg hatching
WP4718: Cholesterol metabolism with Bloch and Kandutsch-Russell pathways
GO:0000904: cell morphogenesis involved in differentiation
GO:0007492: endoderm development
GO:0016071: mRNA metabolic process
GO:0001558: regulation of cell growth
GO:0045596: negative regulation of cell differentiation
R-HSA-194315: Signaling by Rho GTPases
GO:0000460: maturation of 5.8S rRNA
GO:0009725: response to hormone
GO:0010942: positive regulation of cell death
GO:0048729: tissue morphogenesis
GO:0042273: ribosomal large subunit biogenesis
GO:0043408: regulation of MAPK cascade
GO:0000278: mitotic cell cycle

Top 20 enriched GO term of hard gel

Fig. 3: Transcriptome Analysis of hPSCs Cultured on Soft/Hard Gel and Dish(A) Hierarchical Clustering Analysis: Hierarchical clustering analysis of mRNA expression in hPSCs cultured on soft and hard substrates compared to conventional dishes.**(B) Volcano Plot (Soft vs. Dish):** A volcano plot representing the entire gene expression dataset for hPSCs cultured on soft gel vs. dish for 4 days. Red color indicates differentially expressed genes, and dots represent individual genes. Insignificant genes are shown in gray. **(C) Volcano Plot (Hard vs. Dish):** A volcano plot representing the entire gene expression dataset for hPSCs cultured on hard gel vs. dish for 4 days. Red color indicates differentially expressed genes, and dots represent individual genes. Insignificant genes are shown in gray. **(D) Top 20 Gene Ontology (GO) Terms (Soft vs. Dish):** The top 20 Gene Ontology (GO) terms highlighting the categories of up-regulated genes in the cells on soft gel compared to those on dishes. Red boxes highlight terms involved in development.**(E) Top 20 Gene Ontology (GO) Terms (Hard vs. Dish):** The top 20 Gene Ontology (GO) terms highlighting the categories of up-regulated genes in the cells on hard gel compared to those on dishes. Red boxes highlight terms involved in development.

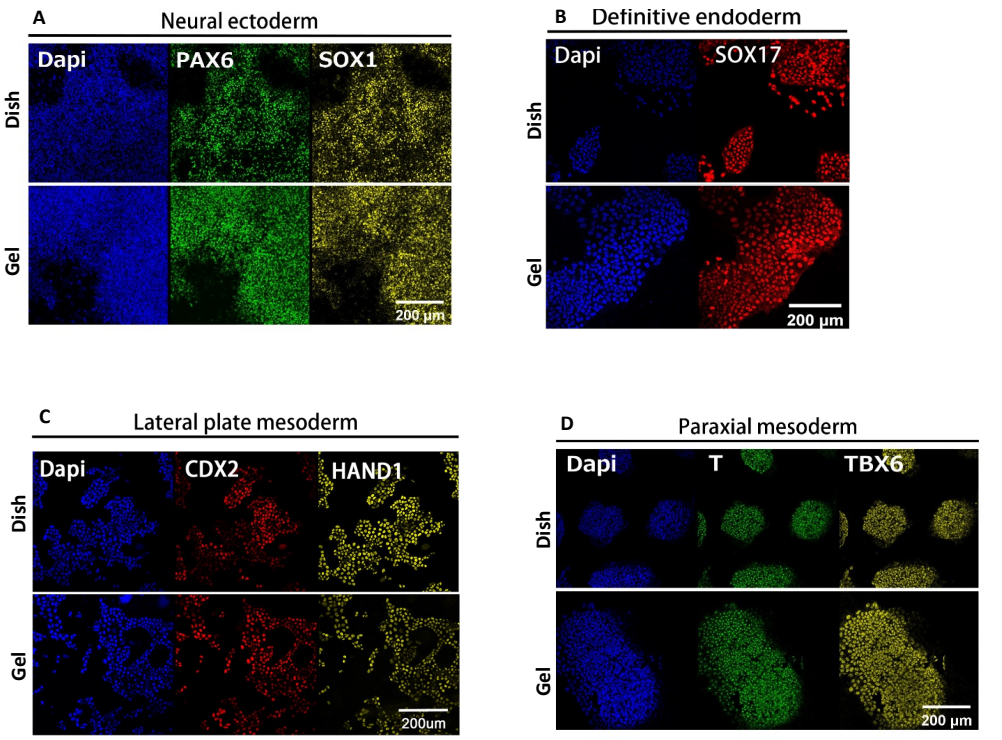

Fig. 4: Immunofluorescent (IF) Staining of Differentiated hPSCs on Hydrogel (A) IF staining of hPSCs undergoing neural ectoderm differentiation on the hydrogel. (B) IF staining of hPSCs undergoing definitive endoderm differentiation on the hydrogel. (C) IF staining of hPSCs undergoing lateral plate mesoderm differentiation on the hydrogel. (D) IF staining of hPSCs undergoing paraxial mesoderm differentiation on the hydrogel. Scale bars: 200 µm.

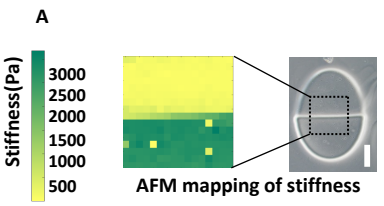

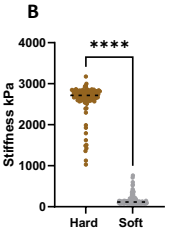

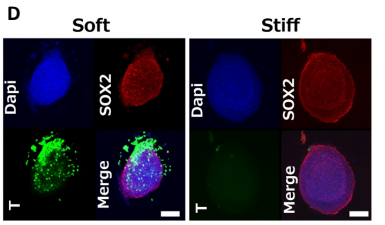

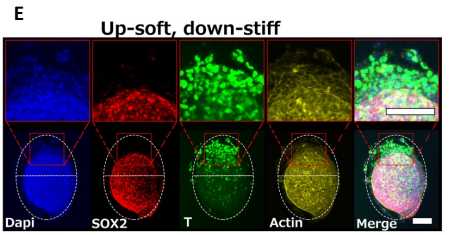

Fig. 5: Spatial Control of Hydrogel Stiffness and Stem Cell Fate(A) Patterned Gel and AFM Stiffness Mapping: Presentation of patterned gel and a heatmap illustrating the surface stiffness of the gel measured by Atomic Force Microscope (AFM). The dotted box indicates the measured region of the hydrogel pattern. **(B) Measured Stiffness of Soft and Hard Regions:** Plot of the measured stiffness values for the soft and hard regions. Each dot represents a measured value, and the dotted line indicates the median value. **(C) Schematic Illustration of Differentiation Method:** A schematic illustration depicting the differentiation method. **(D) IF Staining (Soft vs. Hard Gel):** Immunofluorescent staining of cells differentiated on soft and hard gels using the method shown in Figure 5C. **(E) IF Staining (Partially Soft Gel):** Immunofluorescent staining of cells differentiated on a partially soft gel using the method shown in Figure 5C. The white dotted oval line indicates the whole gel pattern, with the upper half being soft and the lower half being hard. Red boxes show magnified views of the indicated regions. Scale bars: 100 µm. **** $P < 0.0001$ (unpaired, two-tailed t-test).

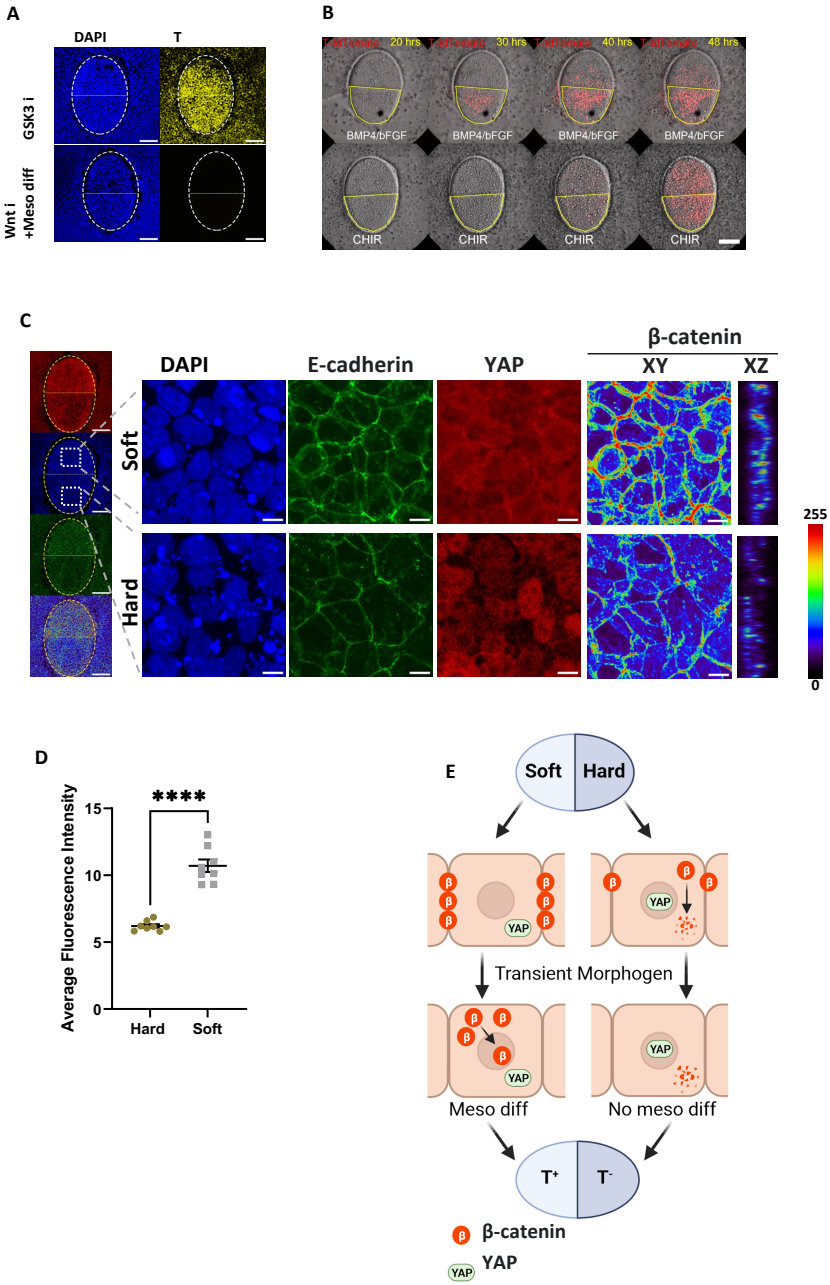

Fig. 6: Speculated Mechanisms of Stem Cell Fate Control

(A) IF Staining (GSK3 Inhibition vs. BMP/bFGF with Wnt Inhibition): Immunofluorescent staining of cells differentiated using GSK3 inhibition or by BMP/bFGF together with Wnt inhibition on a partially soft gel. The white dotted oval line indicates the whole gel pattern, with the upper half being soft and the lower half being hard. Scale bars: 100 µm.

(B) Live Imaging (T-tdTomato Reporter Cell): Screenshot of live imaging of T-tdTomato reporter cells differentiated on a patterned gel using BMP/bFGF or CHIR (Movie 1). The red color represents the tdTomato signal. The yellow line circles the soft part of the gel. Scale bars: 100 µm.

(C) IF Staining (Before Differentiation): Immunofluorescent staining of hPSCs on a partially soft gel pattern before differentiation. The yellow dotted oval line indicates the whole gel pattern, with the upper half being soft and the lower half being hard. The white box indicates a magnified view of the indicated region. The β-catenin channel is shown in XY and XZ section views as a heat map, with colors representing fluorescent intensity. Scale bars: 100 µm in the whole gel view and 10 µm in the magnified view.

(D) Quantification of β-catenin Fluorescent Intensity: Quantification of β-catenin fluorescent intensity based on Z sections of IF staining of the soft and hard regions on the same gel pattern. Each dot represents an individual measurement. The black line shows the mean value. **** $P < 0.0001$ (unpaired, two-tailed t-test). Error bars represent standard deviation.

(E) Proposed Mechanism of Spatial Cell Fate Control: On the soft gel, β-catenin formation is enhanced, and YAP nuclear localization is inhibited, promoting sensitivity to Wnt signaling. On the hard region, cells have nuclear-localized YAP, which negatively impacts Wnt signaling. Together with downregulated β-catenin compared to the soft part, this leads to decreased mesoderm differentiation compared to the soft region.